Received: 25 December 2018

DOI: 10.1002/mma.5850

SPECIAL ISSUE PAPER

WILEY

Fractional-order DOB-sliding mode control for a class of noncommensurate fractional-order systems with mismatched disturbances

Jing Wang[1] | **Changfeng Shao**[1] | **Xiaolu Chen**[1] | **YangQuan Chen**[2]

[1]College of Information Science and Technology, Beijing University of Chemical Technology, Beijing, China

[2]Mechatronics, Embedded Systems and Automation Lab, School of Engineering, University of California, Merced, California

Correspondence
Jing Wang, College of Information Science and Technology, Beijing University of Chemical Technology, Beijing 100029, China.
Email: jwang@mail.buct.edu.cn

Communicated by: D. Zeidan

Funding information
National Natural Science Foundation of China, Grant/Award Number: 61573050; Fundamental Research Funds for the Central Universities of China, Grant/Award Number: XK1802-4

This article proposes a novel fractional-order sliding mode control based on the disturbance observer for a class of noncommensurate fractional-order systems with mismatched disturbances. Firstly, the noncommensurate fractional-order system is decomposed into several subsystems with commensurate order. Then the fractional-order disturbance observers are designed independently to estimate the mismatched disturbances for each subsystems. Based on the designed disturbance observers, a uniform fractional-order sliding mode control is proposed. The proposed method can deal with the mismatched disturbances and has better control performance. The simulations on single-link flexible manipulator system demonstrate the effectiveness of the proposed method.

KEYWORDS

fractional-order disturbance observer, fractional-order sliding mode control, mismatched disturbance, noncommensurate fractional-order systems

MSC CLASSIFICATION

34H05

NOMENCLATURE

A^{-1}	inverse of matrices A
$diag(\dots)$	a square diagonal matrix
$D^{\alpha}f(t)$	the fractional derivative of α order of $f(t)$
$D^{-\alpha}f(t)$	the fractional integral of α order of $f(t)$
$\hat{d}(t)$	the estimation of $d(t)$
R^n	the set of n-dimensional real vectors
$R^{n\times m}$	the set of all $n \times m$ real matrices
Γ	gamma function
$\|\|f(t)\|\|$	2-norm of $f(t)$

1 | INTRODUCTION

As an extension of the classical integer calculus, fractional-order calculus has been developed in the field of theoretical mathematics. It is used to solve complex mathematical processes due to its more special properties. However, in recent years, fractional-order calculus has been widely applied in other fields, such as system modeling, process control, and optimization.[1-3] Fractional calculus is a powerful method to describe data memory and heredity. For example, it is more

accurate to utilize the fractional-order calculus for many physical processes in the modeling domain, such as electrochemical processes,[4] viscoelastic materials,[5] and clinical medicine.[6] In the control strategy research domain, traditional integer-order or differential control strategies have been extended by the introduction of the fractional-order calculus.[7-9] Various fractional-order controllers, such as the fractional-order PID control,[10] fractional-order adaptive control,[11] and fractional-order sliding mode control (FOSMC),[12] can be applied directly to the fractional systems and the integer systems.

It is known that the uncertainties and external disturbances are always inevitable in practical systems. Sliding mode control (SMC) and its improvements, such as adaptive SMC[13] and integral SMC,[14] are useful tools for the fractional (or integer) order systems due to its strong robustness for the matched disturbance. Mujumdar et al[15] proposed an FOSMC for a single-link flexible manipulator. The control law of the proposed FOSMC scheme is designed by using Lyapunov stability analysis approach. However, the common SMC (or FOSMC) has serious chattering problems when dealing the mismatched disturbances. Then the chattering-free control has been further discussed in order to avoid the serious chattering phenomenon in SMC.[16-18] Karami-Mollaee et al[19] proposed a new fractional-order dynamic sliding mode control (FDSMC) for a class of nonlinear systems. An integrator is placed before the input control signal of the plant in order to remove the chattering. Then, a sliding mode observer is presented to extract an appropriate model for the unknown disturbances in the system.

In general, disturbance observer (DOB) is a useful strategy to offset mismatched uncertainty and reduce system chattering in the control strategy of an integer-order system.[20,21] The DOB can estimate the mismatched disturbances that are utilized to compensate the real disturbances in the controller. Zhang et al[22] proposed a DOB-based integral slide mode control approach for continuous-time linear systems with mismatched disturbances or uncertainties. The disturbance estimation can be generated, then it is incorporated into the controller to counteract the disturbances. Li et al[23] developed an SMC approach for systems with mismatched uncertainties via a nonlinear DOB. The DOB-SMC method is developed to counteract the mismatched disturbances by designing a novel sliding surface based on the disturbance estimation. For fractional-order systems, Pashaei and Badamchizadeh[24] designed a new FOSMC based on an integer nonlinear DOB. This approach can reject the effect of mismatched disturbances and has fast and robust stability. Wang et al[12] proposed a FOSMC based on fractional-order DOB for the commensurate fractional-order systems with mismatched disturbances. This method has shown good performance with faster response, lower overshoot, and less chattering effects.

According to the characteristics of the system order, the fractional-order systems can be divided into the commensurate order system and the noncommensurate order system by whether the order of each state is all the same rational number (or the multiple of a rational number). Most researches are focusing on the fractional systems with commensurate order. However, the noncommensurate fractional-order systems show more complicated dynamics than the general commensurate fractional-order system. There is little research on the noncommensurate fractional-order system. So the important issues for noncommensurate fractional-order systems, such as stability analysis and controller design, are less considered. Jiao and Chen[25] analyzed the stability of fractional-order linear time invariant systems with multiple noncommensurate orders. Mujumdar et al[26] investigated an application of fractional theory for control and state estimation for a class of noncommensurate systems. Belkhatir and Laleg-Kirati[27] proposed a two-step algorithm for the joint estimation of parameters and fractional differentiation orders of a linear continuous-time fractional system with noncommensurate orders. This algorithm combines the modulating functions with the first-order Newton methods. Lyapunov stability of linear noncommensurate fractional-order systems is handled in Trigeassou et al,[28] which is based on the concept of fractional energy stored in inductors and capacitor assemblies. Gao[29] focused on a graphical approach to determine the stability of noncommensurate fractional-order systems with time delay. Sabatier et al[30] presented necessary and sufficient condition based on an algorithm that relies on a recursively defined closed-loop realization of the system. The condition can evaluate the stability of the non-commensurate fractional-order systems.

Due to the different orders of the noncommensurate fractional-order system with the mismatched external disturbances, it is difficult to design a universal controller and a unified observer directly. In this paper, a novel method is proposed to simplify this problem. (a) First, the noncommensurate fractional-order system is decomposed into several subsystems with commensurate order. (b) Then, the fractional-order DOBs are independently designed for each subsystem. The novel fractional-order DOBs aim to estimate the mismatched disturbances, and the boundary of the estimation error is theoretically proved to be limited. (c) Finally, the uniform sliding mode controller with all the estimations from the DOBs is implemented to control the overall system.

The reminder of the paper is organized as follows. Section 2 is the problem preliminary in which several preparing issues are discussed, such as the basic definitions and properties of fractional calculus, the model description, and control structure of second-order underactuated noncommensurate fractional-order system. Section 3 proposes the novel fractional-order DOBs and the FOSMC based on these FODOBs, and the estimation effectiveness and the closed-loop

stability are also proven. Section 4 uses the simulations of a single-link flexible manipulator (SLFM) system to verify the validity of the proposed method. Section 5 draws the conclusions.

2 | BASIC KNOWLEDGE AND PROBLEM FORMULATION

2.1 | Basic definitions of fractional calculus

Three definitions of the fractional-order derivatives are most commonly used[31]: the Grünwald-Letnikovs, Riemann-Liouvilles, and Caputos derivative definitions. The Riemann-Liouville's definitions are given here.

Definition 1 (Monje et al[31])**.** The Riemann-Liouville fractional integral of α order of a continuous function $f(t)$ is defined as

$$ {}_{R}D^{-\alpha} f(t) = \frac{1}{\Gamma(\alpha)} \int_{t_0}^{t} f(\tau)(t-\tau)^{\alpha-1} \mathrm{d}\tau, \quad t > t_0, \alpha \in R^{+}, \tag{1} $$

where Γ is the gamma function, which is defined as follows:

$$ \Gamma(q) = \int_{0}^{\infty} x^{q-1} e^{-x} \mathrm{d}x. \tag{2} $$

It should be noted that the fractional integral of order $\alpha > 0$ is represented by $D^{-\alpha}$.

Definition 2 (Monje et al[31])**.** The Riemann-Liouville fractional derivative of α order of a continuous function $f(t)$ is defined as

$$ {}_{R}D^{\alpha} f(t) = \frac{\mathrm{d}^m}{\mathrm{d}t^m} \left[\frac{1}{\Gamma(m-\alpha)} \int_{t_0}^{t} \frac{f(\tau)}{(t-\tau)^{\alpha-m+1}} \mathrm{d}\tau \right], \tag{3} $$

where m is the largest positive integer number satisfying the following condition $m-1 < \alpha < m$.

Property 1. For $\alpha = n$, where n is an integer, the operation $D_t^{\alpha} f(t)$ is the same as the integer-order calculus, ie, $D_t^n f(t) = \frac{d^n}{dt^n} f(t)$, and also, for $\alpha = 0$, we have $D_t^0 f(t) = \frac{d^0}{dt^0} f(t) = f(t)$.

Property 2. The fractional-order integration or differentiation calculus is linear operations, which is similar to the integer-order calculus,

$$ D_t^{\alpha} \left(\lambda f(t) + \mu g(t) \right) = \lambda D_t^{\alpha} f(t) + \mu D_t^{\alpha} g(t). \tag{4} $$

Property 3. For the arbitrary fractional-order, $\alpha > 0, \beta > 0, \beta \in (m-1, m)$, n is integer, the following equalities hold for the hybrid fractional derivative and integral operation,

$$ \frac{d^n}{dt^n} \left(D_t^{\beta} f(t) \right) = D_t^{\alpha+\beta} f(t), \tag{5} $$

$$ D_t^{\alpha} \left(D_t^{-\beta} f(t) \right) = D_t^{\alpha-\beta} f(t), \tag{6} $$

$$ D_t^{-\alpha} \left(D_t^{\beta} f(t) \right) = D_t^{-\alpha+\beta} f(t) - \sum_{j=1}^{m} \left[D_t^{\beta-j} f(t) \right]_{t=t_0} \frac{(t-t_0)^{\alpha-j}}{\Gamma(1+\alpha-j)}. \tag{7} $$

Lemma 1. *For an integrable function f(t), if there is at least one $t_1 \in (0, t)$ such that $f(t_1) \neq 0$, then there is a positive constant N such that $D^{-\alpha} |f(t)| \geq N$.*

2.2 | Problem formulation

The general noncommensurate fractional-order system can be represented by the following differential equation,[33]

$$ \begin{aligned} &D^{\alpha n} y(t) + a_{n-1} D^{\beta(n-1)} y(t) + a_{n-2} D^{\gamma(n-2)} y(t) + \ \dots \ + a_0 y^{\delta}(t) \\ &\quad = b_m D^{\mu m} u(t) + b_{m-1} D^{\nu(m-1)} u(t) + \ \dots \ + b_0 u^{\eta}(t), \end{aligned} \tag{8} $$

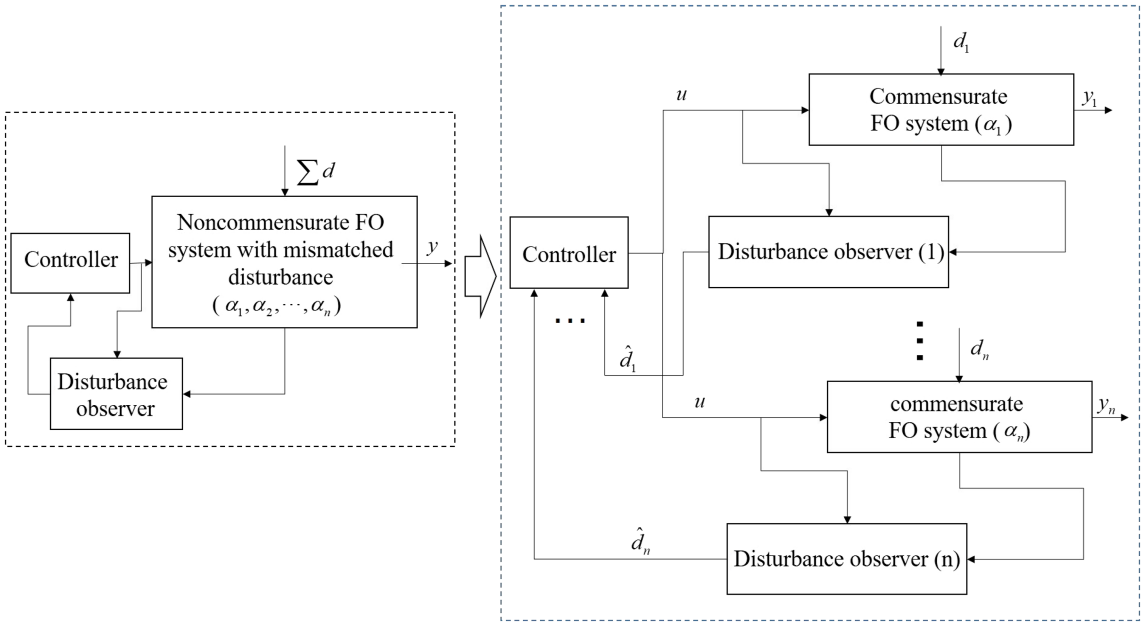

FIGURE 1 The design diagram of noncommensurate fractional-order system [Colour figure can be viewed at wileyonlinelibrary.com]

where the fractional orders $\alpha, \beta, \gamma, \ldots, \delta$ are different in the noncommensurate situation.

A fractional-order DOB-based SMC method is proposed for a class of noncommensurate fractional-order systems with mismatched disturbances. The design diagram is described in Figure 1. The specific operations of decomposing into subsystems are as follows: the variables with the same fractional calculus in the original system are respectively composed into one subsystem. For example, if the original system has n state variables, $x_1, \ldots, x_n$. They have three different orders of α, β, and γ. Then the original system can be decomposed into three subsystems whose order are α, β, and γ, respectively.

In this paper, a noncommensurate fractional-order system with two different orders is considered.

$$\begin{cases} D^{\beta} z_1 = A_{11} z_1 + A_{12} z_2 + B_{d_1} d_1 \\ D^{\alpha} z_2 = A_{21} z_1 + A_{22} z_2 + B_2 u + B_{d_2} d_2 \\ y = C_1 z_1, \end{cases} \tag{9}$$

where $\alpha, \beta \in (0, 1)$ are the different orders of the system, $z_1(t) \in R^{n_1 \times 1}, z_2(t) \in R^{n_2 \times 1}$ are the state variables, $u(t) \in R^m$ is the control signal, $y(t) \in R^p$ is the output, and $d_1(t) \in R^1$ and $d_2(t) \in R^1$ are the mismatched external disturbances. $A_{11} \in R^{n_1 \times n_1}, A_{12} \in R^{n_1 \times n_2}, A_{21} \in R^{n_2 \times n_1}$ and $A_{22} \in R^{n_2 \times n_2}$ are the state matrices. $B_2 \in R^{n_2 \times m}$ is the control matrix. $B_{d_1} \in R^{n_1 \times 1}, B_{d_2} \in R^{n_2 \times 1}$ are the disturbance matrix. Since the control matrix B_2 is inconsistent with the coefficient matrix B_{d1} and B_{d2} of the disturbance, so these disturbances are mismatch. $C_1 \in R^{p \times n_1}$ is the output matrix.

Assumption 1. The mismatched disturbances $d_1(t)$ and $d_2(t)$ are bounded, $\|d_1(t)\| \leq \varepsilon_1$, $\|d_2(t)\| \leq \varepsilon_2$, where ε_1 and ε_2 are positive constants.

As we all known, if $d_1(t)$ or $d_2(t)$ is a white noise, the use of advanced control technology such as DOB is not satisfactory. For the noncommensurate fractional-order system (9) with the mismatched disturbances, the controller $u(t)$ is designed to make the output asymptotically track the desired reference $y_d(t)$ in a finite time, and the tracking error is close to zero without any effect from the external mismatched disturbances.

3 | DESIGN OF FOSMC

For the noncommensurate fractional-order system (8), it is difficult to design a DOB and estimate the disturbances directly. Therefore, we decompose the system (8) into two subsystems with the same orders as shown in (9), and then design the DOB, respectively.

3.1 | Fractional-order DOB

First, a new fractional-order DOB for $d_1(t)$ is designed as follows:

$$\begin{cases} D^{1+\alpha}p_1(t) = -L_1B_{d_1}\left(D^{\alpha}p_1(t) + L_1D^{\alpha+\beta-1}z_1(t)\right) \\ \qquad\qquad - L_1D^{\alpha}\left(A_{11}z_1(t) + A_{12}z_2(t)\right) \\ \qquad\qquad D^{\alpha}\hat{d}_1(t) = D^{\alpha}p_1(t) + L_1D^{\alpha+\beta-1}z_1(t). \end{cases} \tag{10}$$

The DOB for disturbance $d_2(t)$ is designed as

$$\begin{cases} \dot{p}_2(t) = -L_2B_{d_2}\left(p_2(t) + LD^{\alpha-1}z_2(t)\right) \\ \qquad\qquad - L_2\left(A_{21}z_1(t) + A_{22}z_2 + B_2u(t)\right) \\ \qquad\qquad \hat{d}_2(t) = p_2(t) + L_2D^{\alpha-1}z_2(t), \end{cases} \tag{11}$$

where $\hat{d}_1(t)$ and $\hat{d}_2(t)$ are the estimations of the disturbances $d_1(t)$ and $d_2(t)$, $p_1(t)$and$p_2(t)$ are the auxiliary vectors of the observers, and L_1andL_2 are the gain matrices of the observers. The design of L_1andL_2 should satisfy that $-L_1B_{d_1}$ and $-L_2B_{d_2}$ are Hurwitz. The estimation errors of $d_1(t)$ and $d_2(t)$ are

$$\begin{aligned} e_{d_1}(t) &= d_1(t) - \hat{d}_1(t), \\ e_{d_2}(t) &= d_2(t) - \hat{d}_2(t). \end{aligned} \tag{12}$$

The fractional-order calculus of the estimation error $e_{d_1}(t)$ is defined as

$$D^{\alpha}e_{d_1}(t) = D^{\alpha}d_1(t) - D^{\alpha}\hat{d}_1(t). \tag{13}$$

Lemma 2. *Assume A is Hurwitz and has n distinct eigenvalues. Let X be a nonsingular matrix such that $XAX^{-1} = diag\,(\lambda_1, \ldots \lambda_n)$. There exists an positive constant σ such that*

$$\left\|e^{At}\right\| \le \sigma e^{\lambda_{\max}(A)t}, \tag{14}$$

where $\sigma = \left\|X^{-1}\right\| \|X\|$.

Theorem 1. *For the proposed fractional-order DOBs (10) and (11), the estimation errors $D^{\alpha}e_{d_1}(t)$ and $e_{d_2}(t)$ are bounded and satisfy*

$$\left\|D^{\alpha}e_{d_1}(t)\right\| \le \gamma, \tag{15}$$

$$\left\|e_{d_2}(t)\right\| \le \lambda, \tag{16}$$

where γ and λ are a positive scalar.

Proof. First consider the disturbance $d_1(t)$, according to (10) and (13), we have

$$\begin{aligned} \frac{\mathrm{d}}{\mathrm{d}t}D^{\alpha}e_{d_1}(t) &= D^{\alpha+1}d_1(t) - D^{\alpha+1}\hat{d}_1(t) \\ &= D^{\alpha+1}d_1(t) - D^{1+\alpha}p_1(t) - L_1D^{\alpha+\beta}z_1(t) \\ &= D^{\alpha+1}d_1(t) + L_1B_{d_1}\left(D^{\alpha}p_1(t) + L_1D^{\alpha+\beta-1}z_1(t)\right) \\ &\quad + L_1D^{\alpha}\left(A_{11}z_1(t) + A_{12}z_2(t)\right) - L_1D^{\alpha+\beta}z_1(t) \\ &= D^{\alpha+1}d_1(t) + L_1B_{d_1}D^{\alpha}\hat{d}(t) + L_1D^{\alpha}\left(A_{11}z_1(t) + A_{12}z_2(t)\right) \\ &\quad - L_1D^{\alpha}\left(A_{11}z_1(t) + A_{12}z_2(t)\right) - L_1B_{d_1}D^{\alpha}d_1(t) \\ &= D^{\alpha+1}d_1(t) - L_1B_{d_1}D^{\alpha}e_{d_1}(t). \end{aligned} \tag{17}$$

Define $M_1 = -L_1 B_{d_1}$, and $d_{1new}(t) = D^\alpha d_1(t)$, so $e_{d_{1new}}(t) = D^\alpha e_{d_1}(t)$, then (17) can be written as

$$\dot{e}_{d_{1new}}(t) = \dot{d}_{1new}(t) + M_1 e_{d_{1new}}(t). \tag{18}$$

Taking the integration of (18) gives

$$e_{d_{1new}}(t) = e^{M_1 t} e_{d_{1new}}(0) + \int_0^t e^{M_1(t-\tau)} M \dot{d}_{1new}(\tau) \mathrm{d}\tau. \tag{19}$$

Based on the RLs derivative definition and Assumption 1,

$$\begin{aligned} \|d_{1new}(t)\| &= \|D^\alpha d(t)\| \\ &= \left\| \frac{\mathrm{d}}{\mathrm{d}t} \left[\frac{1}{\Gamma(1-\alpha)} \int_0^t (t-\tau)^{-\alpha} d_1(\tau) \mathrm{d}\tau \right] \right\| \\ &= \left\| \frac{1}{\Gamma(1-\alpha)} \right\| \left\| \int_0^t (-\alpha)(t-\tau)^{-1-\alpha} d_1(\tau) \mathrm{d}\tau \right\| \\ &\le \left\| \frac{1}{\Gamma(1-\alpha)} \right\| \|d_1(t)\| \left\| \int_0^t (-\alpha)(t-\tau)^{-1-\alpha} \mathrm{d}\tau \right\| \\ &= \left\| \frac{\varepsilon_1(-\alpha)}{\Gamma(1-\alpha)} \right\| \left\| \int_0^t (t-\tau)^{-1-\alpha} \mathrm{d}\tau \right\|. \end{aligned} \tag{20}$$

Define $\delta = \left\| \frac{\varepsilon_1(-\alpha)}{\Gamma(\beta-\alpha)} \right\| \left\| \int_0^t (t-\tau)^{-1-\alpha} \mathrm{d}\tau \right\|$, where δ is a positive scalar. Thus, we have $\|d_{1\mathrm{new}}(t)\| \le \delta$. Then,

$$\begin{aligned} &\left\| e_{d_{1new}}(t) \right\| \\ &\le \left\| e^{M_1 t} e_{d_{1new}}(0) \right\| + \left\| \int_0^t e^{M_1(t-\tau)} \dot{d}_{1new}(\tau) d\tau \right\| \\ &\le \left\| e^{M_1 t} \right\| \left\| e_{d_{1new}}(0) \right\| + \left\| e^{M_1(t-\tau)} d_{1new}(\tau) \Big|_0^t + M_1 \int_0^t e^{M_1(t-\tau)} d_{1new}(\tau) \mathrm{d}\tau \right\| \\ &\le \sigma e^{\lambda_{\max}(M_1)t} \left\| e_{d_{1new}}(0) \right\| + \left\| \left\| d_{1new}(t) - e^{M_1 t} d_{1new}(0) \right\| + M_1 \int_0^t \left\| e^{M_1(t-\tau)} \right\| \|d_{1new}(\tau)\| \, \mathrm{d}\tau \right\| \\ &\le \sigma e^{\lambda_{\max}(M_1)t} \left\| e_{d_{1new}}(0) \right\| + \left\| \|d_{1new}(t)\| + \left\| e^{M_1 t} d_{1new}(0) \right\| + M_1 \sigma \delta \int_0^t \left\| e^{\lambda_{\max}(M_1)(t-\tau)} \right\| \mathrm{d}\tau \right\| \\ &\le \sigma e^{\lambda_{\max}(M_1)t} \left\| e_{d_{1new}}(0) \right\| + \left\| \delta + \left\| e^{M_1 t} d_{1new}(0) \right\| + M_1 \sigma \delta \frac{1}{\lambda_{\max}(M_1)} \left(e^{\lambda_{\max}(M_1)t} - 1 \right) \right\|. \end{aligned} \tag{21}$$

M_1 is Hurwitz matrix, so $Re\lambda_{\max}(M_1) < 0$, $e^{\lambda_{\max}(M_1)t} \le 1$. Then,

$$\begin{aligned} \left\| e_{d_{1new}}(t) \right\| &\le \sigma \left\| e_{d_{1new}}(0) \right\| + \delta + \|d_{1new}(0)\| \\ &\quad + \left\| M_1 \sigma \delta \frac{1}{\lambda_{\max}(M_1)} \left(e^{\lambda_{\max}(M_1)t} - 1 \right) \right\| \\ &\le \sigma \left\| e_{d_{1new}}(0) \right\| + \delta + \|d_{1new}(0)\| + \left\| M_1 \sigma \delta \frac{1}{\lambda_{\max}(M_1)} \right\|. \end{aligned} \tag{22}$$

Define $\gamma = \sigma \left\| e_{d_{1new}}(0) \right\| + \delta + \|d_{1new}(0)\| - M_1 \sigma \delta \frac{1}{\lambda_{\max}(M_1)}$ and take it into (22), the (15) can be immediately obtained.

Similarly, the proof about the estimation error (16) for the disturbance $d_2(t)$ can be obtained. Thus, the proof of Theorem 1 is completed. □

3.2 | Fractional-order SMC

In this section, a novel DOB-FOSMC is proposed for the noncommensurate fractional-order system (9). The tracking error is $e(t) = y(t) - y_d(t)$ when the target value of the output $y(t)$ is $y_d(t)$.

The fractional-order sliding surface for the given system (9) is designed as

$$s = a_1 e + a_2 D^{\alpha+\beta-1} e, \tag{23}$$

where a_1 and a_2 are designed parameters and α and β are the orders of the system.

The fractional-order sliding mode reaching law can be calculated by

$$u_r(t) = -\frac{1}{a_2}(C_1 A_{12} B_2)^{-1} \left(k_1 s + k_2 sign(s)\right), \tag{24}$$

where k_1 and k_2 are constant gains.

In order to satisfy the sliding condition in the presence of the mismatched disturbances, the equivalent control law is

$$\begin{aligned} u_{eq}(t) = &-(C_1 A_{12} B_2)^{-1} \left(C_1 A_{12} \left(A_{21} z_1 + A_{22} z_2 + B_{d_2} \hat{d}_2\right)\right. \\ &\left. + D^{\alpha} C_1 \left(A_{11} z_1 + B_{d_1} \hat{d}_1\right) + (C_1 A_{12} B_2)^{-1} \left(D^{\alpha+\beta} y_d - \frac{a_1}{a_2} \dot{e}\right)\right). \end{aligned} \tag{25}$$

The FOSMC law is

$$\begin{aligned} u(t) &= u_{eq}(t) + u_r(t) \\ &= -(C_1 A_{12} B_2)^{-1} \left(C_1 A_{12} \left(A_{21} z_1 + A_{22} z_2 + B_{d_2} \hat{d}_2\right) + D^{\alpha} C_1 \left(A_{11} z_1 + B_{d_1} \hat{d}_1\right)\right) \\ &\quad + (C_1 A_{12} B_2)^{-1} \left(D^{\alpha+\beta} y_d - \frac{a_1}{a_2} \dot{e}\right) - \frac{1}{a_2}(C_1 A_{12} B_2)^{-1} \left(k_1 s + k_2 sign(s)\right). \end{aligned} \tag{26}$$

Theorem 2. *For the general system (9), design the fractional-order sliding surface (23) and the controller (26). Then the closed-loop system with observers estimations (10) and (11) is stable. The output variable $y(t)$ can asymptotically track the reference $y_d(t)$ under the influence of the mismatched disturbance in finite time.*

Proof. The Lyapunov function is defined as

$$V = \frac{1}{2} s^2. \tag{27}$$

From the fractional-order sliding surface (23), we have

$$\begin{aligned} \dot{s}(t) &= a_1 \dot{e} + a_2 D^{\alpha+\beta-1} \dot{e} \\ &= a_1 \dot{e} + a_2 D^{\alpha+\beta} (y - y_d) \\ &= a_1 \dot{e} + a_2 D^{\alpha+\beta} C_1 z_1 - a_2 D^{\alpha+\beta} y_d \\ &= a_1 \dot{e} + a_2 D^{\alpha} C_1 \left(A_{11} z_1 + A_{12} z_2 + B_{d_1} d_1\right) - a_2 D^{\alpha+\beta} y_d \\ &= a_1 \dot{e} + a_2 C_1 A_{12} \left(A_{21} z_1 + A_{22} z_2 + B_2 u + B_{d_2} d_2\right) \\ &\quad + a_2 D^{\alpha} C_1 \left(A_{11} z_1 + B_{d_1} d_1\right) - a_2 D^{\alpha+\beta} y_d. \end{aligned} \tag{28}$$

Then the time derivative of (27) is

$$\begin{aligned}
\dot{V} &= s\dot{s} \\
&= s\left(a_1\dot{e} + a_2C_1A_{12}\left(A_{21}z_1 + A_{22}z_2 + B_2u + B_{d_2}d_2\right) + a_2D^{\alpha}C_1\left(A_{11}z_1 + B_{d_1}d_1\right) - a_2D^{\alpha+\beta}y_d\right) \\
&= s\left(a_1\dot{e} + a_2C_1A_{12}\left(A_{21}z_1 + A_{22}z_2 + B_2\left((C_1A_{12}B_2)^{-1}\left(\left(D^{\alpha+\beta}y_d - a_1\dot{e}/a_2\right)\right.\right.\right.\right. \\
&\quad \left.\left.\left.\left.-C_1A_{12}\left(A_{21}z_1 + A_{22}z_2 + B_{d_2}\hat{d}_2\right) - D^{\alpha}C_1\left(A_{11}z_1 + B_{d_1}\hat{d}_1\right) - {}^{(k_1s+k_2sign(s))}/_{a_2}\right)\right.\right. \right. \\
&\quad \left.\left.\left.+(C_1A_{12}B_2)^{-1}\left(D^{\alpha+\beta}y_d - {}^{a_1}/_{a_2}\dot{e}\right)\right) + B_{d_2}d_2\right) + a_2D^{\alpha}C_1\left(A_{11}z_1 + B_{d_1}d_1\right) - a_2D^{\alpha+\beta}y_d\right) \\
&= s\left(a_2C_1\left(B_{d_1}D^{\alpha}\left(d_1 - \hat{d}_1\right) + A_{12}B_{d_2}\left(d_2 - \hat{d}_2\right)\right) - \left(k_1s + k_2sign(s)\right)\right) \\
&\le -k_1s^2 - \left(k_2 - a_2C_1\left(B_{d_1}D^{\alpha}e_{d_1} + A_{12}B_{d_2}e_{d_2}\right)\right)|s|\,.
\end{aligned} \tag{29}$$

In Section 3.1, $\left\|D^{\alpha}e_{d_1}(t)\right\| \le \gamma$ and $\left\|e_{d_2}(t)\right\| \le \lambda$ are proved. According to (28) and observers (10) and (11), if $k_1 \ge 0$, $k_2 \ge a_2\left(C_1B_{d_1}\gamma + C_1A_{12}B_{d_2}\lambda\right)$, then $\dot{V} \le 0$, which implies that the sliding surface can be attained in finite time.

The reaching time is calculated in the following:

$$\begin{aligned}
\dot{V}(t) &\le -k_1s^2 - \left(k_2 - a_2C_1\left(B_{d_1}D^{\alpha}e_{d_1} + A_{12}B_{d_2}e_{d_2}\right)\right)|s| \\
\dot{V}(t) &\le -\left(k_2 - a_2C_1\left(B_{d_1}\gamma + A_{12}B_{d_2}\lambda\right)\right)|s|
\end{aligned}\,. \tag{30}$$

Taking the fractional integral α of (29) gives

$$\begin{aligned}
&D^{1-\alpha}V(t_r) - V(0)\frac{(t_r)^{\alpha-1}}{\Gamma(\alpha)} \\
&\quad \le -\left(k_2 - a_2C_1\left(B_{d_1}\gamma + A_{12}B_{d_2}\lambda\right)\right)D^{-\alpha}|s|\,,
\end{aligned} \tag{31}$$

where t_r is the reaching time.

Based on Lemma 1 and $V(t_r) = 0$, (30) is

$$\begin{aligned}
&-V(0)\frac{(t_r)^{\alpha-1}}{\Gamma(\alpha)} \le -\left(k_2 - a_2C_1\left(B_{d_1}\gamma + A_{12}B_{d_2}\lambda\right)\right)N \\
&(t_r)^{\alpha-1} \ge \frac{\Gamma(\alpha)\left(k_2 - a_2C_1\left(B_{d_1}\gamma + A_{12}B_{d_2}\lambda\right)\right)N}{V(0)} \\
&\frac{1}{(t_r)^{1-\alpha}} \ge \frac{\Gamma(\alpha)\left(k_2 - a_2C_1\left(B_{d_1}\gamma + A_{12}B_{d_2}\lambda\right)\right)N}{V(0)} \\
&t_r \le \left(\frac{V(0)}{\Gamma(\alpha)\left(k_2 - a_2C_1\left(B_{d_1}\gamma + A_{12}B_{d_2}\lambda\right)\right)N}\right)^{\frac{1}{1-\alpha}}.
\end{aligned} \tag{32}$$

Thus, the tracking error of output variables will converge to zero in the finite time. □

4 | SIMULATION RESULTS

To evaluate and verify the efficiency and excellent properties of the proposed FODOB-based FOSMC, a SLFM system is selected for simulation. Due to the flexible nature of the link, when an reference angle θ is given at motor end, the tip end will bring an angle φ. The angle φ in tip end is too small to be approximated as $\varphi = \frac{D}{L}$, where L is the length

of the link and D is the displacement of tip. The dynamic equation of the system can be obtained by Euler Lagrange equation.[35]

$$\begin{cases} \ddot{\theta} = \dfrac{T_1}{J_{eq}} - \dfrac{B_{eq}\dot{\theta}}{J_{eq}} + \dfrac{K_{stiff}\phi}{J_{eq}} \\ \ddot{\phi} = -K_{stiff}\left(\dfrac{1}{J_{link}} + \dfrac{1}{J_{eq}}\right)\phi + \dfrac{B_{eq}}{J_{eq}}\dot{\theta} - \dfrac{T_1}{J_{eq}} \end{cases} . \tag{33}$$

The physical meaning and value of each parameter can be obtained from Kurode and Dixit.[36]

Define $x_1 = \theta, x_2 = \phi, x_3 = \dot{\theta}, x_4 = \dot{\phi}$. Mujumdar et al[26] proposed the noncommensurate fractional-order flexible link manipulator system. Considering the modeling error and external disturbance of the motor end and tip end, the following flexible link manipulator system can be obtained.

$$\begin{cases} D^{\beta}x_1 = x_3 + a_1 d_1 \\ D^{\beta}x_2 = x_4 + a_2 d_1 \\ D^{\alpha}x_3 = 936.39x_2 - 41.19x_3 + 72.4593u + a_3 d_2 \\ D^{\alpha}x_4 = -1372.6x_2 + 41.19x_3 - 72.4593u + a_4 d_2 \\ y = x_1 \end{cases} . \tag{34}$$

where α and β are fractions < 1.

In order to obtain the parameters of noncommensurate fractional-order flexible link manipulator system, experiments were carried out in Mujumdar et al.[26] The plant was excited by square-wave input with frequency 1.5 Hz and amplitude 0.1. Then, vibrations of the link were noted. The models (both integer and proposed fractional) were also excited by the same input, and link vibrations from models were compared with experimental output. Orders of the fractional model are fixed in a noncommensurate manner to get similar performance as that of the actual plant. During this experimentation, the values of α and β were obtained as $\alpha = 0.71$ and $\beta = 0.92$.

Then it is equivalent to

$$\begin{cases} D^{\beta}z_1 = z_2 + B_{d_1}d_1 \\ D^{\alpha}z_2 = A_{21}z_1 + A_{22}z_2 + B_2 u + B_{d_2}d_2 \\ y = C_1 z_1 \end{cases} , \tag{35}$$

where $z_1 = [x_1, x_2]^T$, $z_2 = [x_3, x_4]^T$, $\alpha = 0.71$, $\beta = 0.92$, $A_{21} = \begin{bmatrix} 0 & 936.39 \\ 0 & -1372.6 \end{bmatrix}$, $A_{22} = \begin{bmatrix} -41.19 & 0 \\ 41.19 & 0 \end{bmatrix}$, $B_{d_1} = \begin{bmatrix} 1 \\ 1 \end{bmatrix}$, $B_{d_2} = \begin{bmatrix} 1 \\ 1 \end{bmatrix}$, $B_2 = \begin{bmatrix} 72.4593 \\ -72.4593 \end{bmatrix}$, $C_1 = \begin{bmatrix} 1 & 0 \end{bmatrix}$.

Consider the tracking setting curves of output are step functions with amplitude 20. Suppose the disturbances $d_1 = 10\sin(4\pi t), d_2 = 15\sin(2\pi t)$. The parameters of the controller and observer are listed as follows: $a_1 = 10, a_2 = 1, k_1 = 30, k_2 = 10, \alpha = 0.71, \beta = 0.92, L_1 = \begin{bmatrix} 10 & 100 \end{bmatrix}, L_2 = \begin{bmatrix} 10 & 50 \end{bmatrix}$.

The controller is

$$\begin{aligned} u(t) &= u_{eq}(t) + u_r(t) \\ &= (C_1B_2)^{-1}\left(\left(D^{1.63}y_d - 10\dot{e}\right) - C_1\left(A_{21}z_1 + A_{22}z_2 + B_{d_1}D^{0.71}\hat{d}_1 + B_{d_2}\hat{d}_2\right)\right) \\ &\quad - (C_1B_2)^{-1}(30s + 2sign(s)) \end{aligned} . \tag{36}$$

The sliding surface is

$$s(t) = 10e_y(t) + D^{0.63}e_y(t). \tag{37}$$

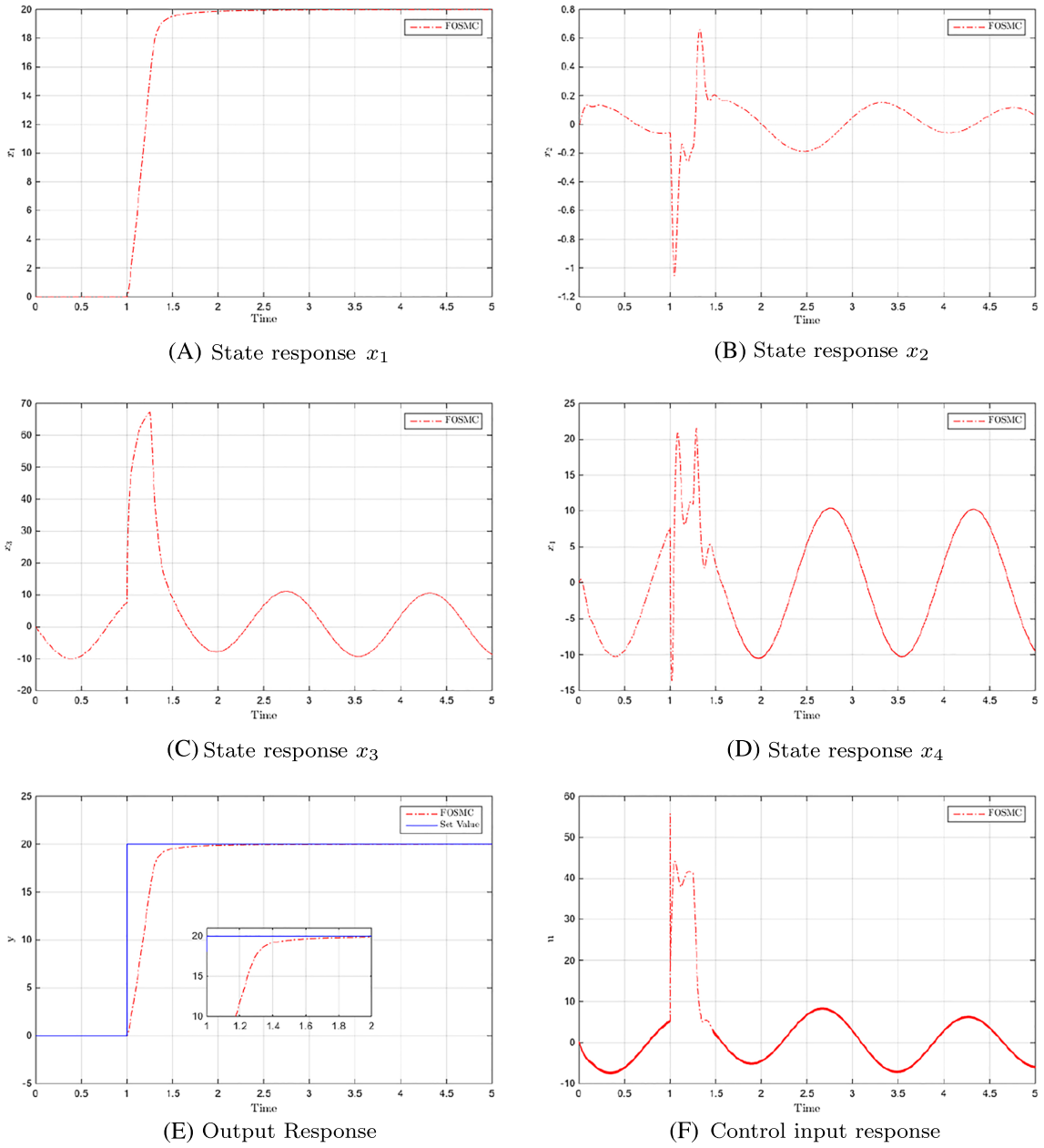

FIGURE 2 Response curves of fractional-order (FO)-single-link flexible manipulator (SLFM) system [Colour figure can be viewed at wileyonlinelibrary.com]

The Oustaloup recursive filter and the modified version presented in Monje et al[31] are used to evaluate fractional-order differentiations during the simulation. Generally speaking, Oustaloups approximation to fractional-order operators are good enough in most cases. A MATLAB object FOTF toolbox is used to actualize the approximate calculation of fractional order (FO) differentiations and system simulations. The solution steps can be basically divided into the following five steps:

Step 1: Initialize state variables and parameters of the system.
Step 2: Design the observer (10), the estimated values $\hat{d}_1$ and $\hat{d}_2$ are obtained by using FODOB.
Step 3: Design the sliding mode controller (26) and calculate the deviation e and sliding surface s (23).
Step 4: Update the status and output of the system.
Step 5: Repeat steps 2 to 4 until the deviation e reaches a stable value.

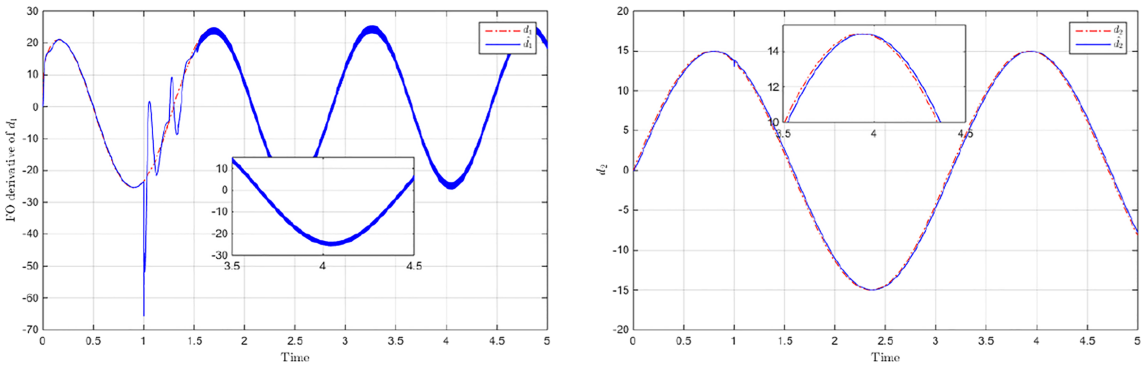

(A) State response d_1 (B) State response d_2

FIGURE 3 Comparison of actual and estimate disturbance [Colour figure can be viewed at wileyonlinelibrary.com]

The simulation results are shown in Figures 2 and 3. Figure 2A-F represents the four-state response curves, control input curves, and output curves, respectively. The four states indicate the deflection angle in motor end and tip end, deflection angle acceleration in motor end and tip end, respectively. From Figure 2A-F, we can see that the output of the system can track the reference value very well even in the case of mismatched interference, and it has a fast response ($t_s < 0.5$ second). The chattering effect of the steady-state process is well suppressed (almost zero). Due to the faster response, it can be seen that the angular accelerations in Figure 2C,D have drastic changes. Under the influence of disturbance, considering the physical characteristics of the flexible rod, it can be seen from Figure 2B that the angular displacement in the tip end will produce certain fluctuations with a fluctuation range ($\pm 0.2°$), and this fluctuation is within an acceptable range.

Figure 3 shows the response curves of the mismatched disturbances d_1 and d_2 and their estimations, where the blue solid line is the true value of the disturbance and the red dotted line represents the estimation of the DOB. It can be clearly seen from Figure 3 and its partial enlargement that the observers proposed in this paper can accurately estimate the mismatched disturbance of the system.

Then, we compare the simulation of the fractional-order flexible link manipulator system (35) with integer-order SMC and FOSMC.

The integer-order sliding mode controller (IOSMC) is

$$\begin{aligned} u(t) &= u_{eq}(t) + u_r(t) \\ &= (C_1B_2)^{-1}\left((\ddot{y}_d - 10\dot{e}) - C_1\left(A_1z_1 + A_2z_2 + B_{d_1}\dot{\hat{d}}_1 + B_{d_2}\hat{d}_2\right)\right) \\ &\quad - (C_1B_2)^{-1}(30s + 2sign(s)) \end{aligned} \quad . \tag{38}$$

The sliding surface of IOSMC is

$$s(t) = 10e_y(t) + \dot{e}_y(t). \tag{39}$$

The compared simulation results of two methods, IOSMC and FOSMC, are shown in Figure 4. Here, for simplicity, IOSMC is shorten as SMC.

Figure 4A-F represents the state, the control input, and the output response curves of FO-SLFM system. It can be seen that the output of the system can track the reference value well by using the two methods. We focus on the output response Figure 4E and control input Figure 4F of the system. It can be seen from the partial enlargement graphs that the FOSMC has faster response from Figure 4E. It is found from Figure 4F that FOSMC gives more improvement in the effect of disturbance rejection than the traditional integer-order SMC.

In order to further explain the superiority of the proposed method, we apply the integer-order SMC for the classical integer-order flexible link manipulator system as the comparison method. The compared simulation results are shown in Figure 5. A running time table of the procedures (corresponding to Figures 2, 4, and 5) is given in Table 1. All of the procedures run short enough to not burden the computational complexity.

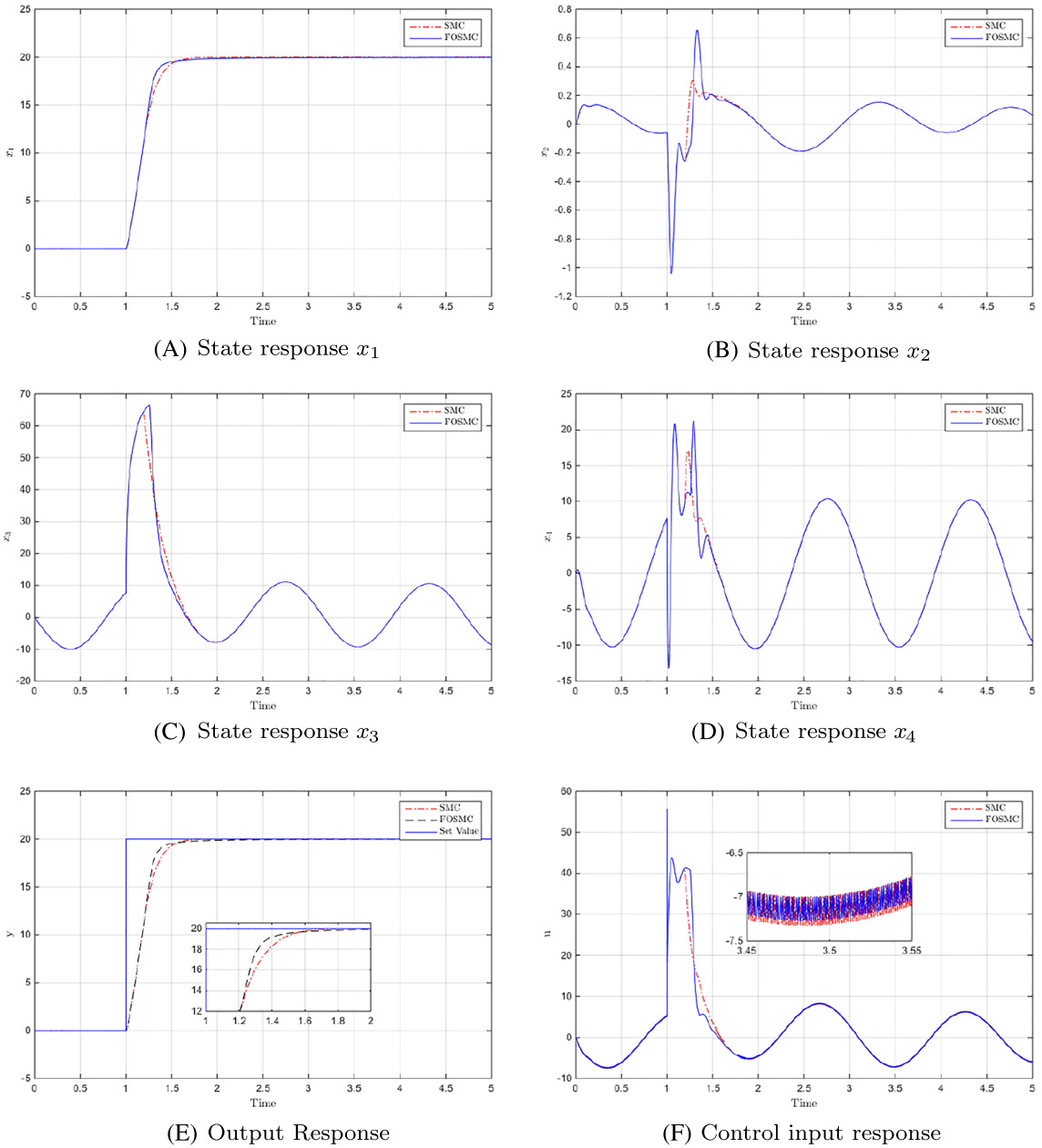

FIGURE 4 Response comparison of FO-SLFM system with SMC and FOSMC. FO, fractional order; FOSMC, fractional-order sliding mode control; SLFM, single-link flexible manipulator; SMC, sliding mode control [Colour figure can be viewed at wileyonlinelibrary.com]

Figure 5A-F represents the state, the control input, and the output response curves of IO-SLFM and FO-SLFM system. It can be seen that the output of the system can track the reference value well by using the two methods. However, the integer-order control method is slightly inadequate in reducing the chattering and suppressing the disturbance. From the partial enlargement graphs of Figure 5A and Figure 5E, it can be seen that the convergence rate of fractional-order control method is slightly improved. Moreover, the chattering and external disturbances can be better suppressed in the steady-state process. From Figure 5B,E, it is found that there is a significant difference between the control input and the angular displacement in tip end. The control input of the integer-order control method has an intense chattering, while the control input of the fractional-order control method is almost smooth. The integer-order control method produces a violent chattering effect in the angle displacement in the tip end. The amplitude is about 7%, which is much larger than that of the fractional-order system. It shows the excellent performance of the FOSMC method with DOB proposed in this paper.

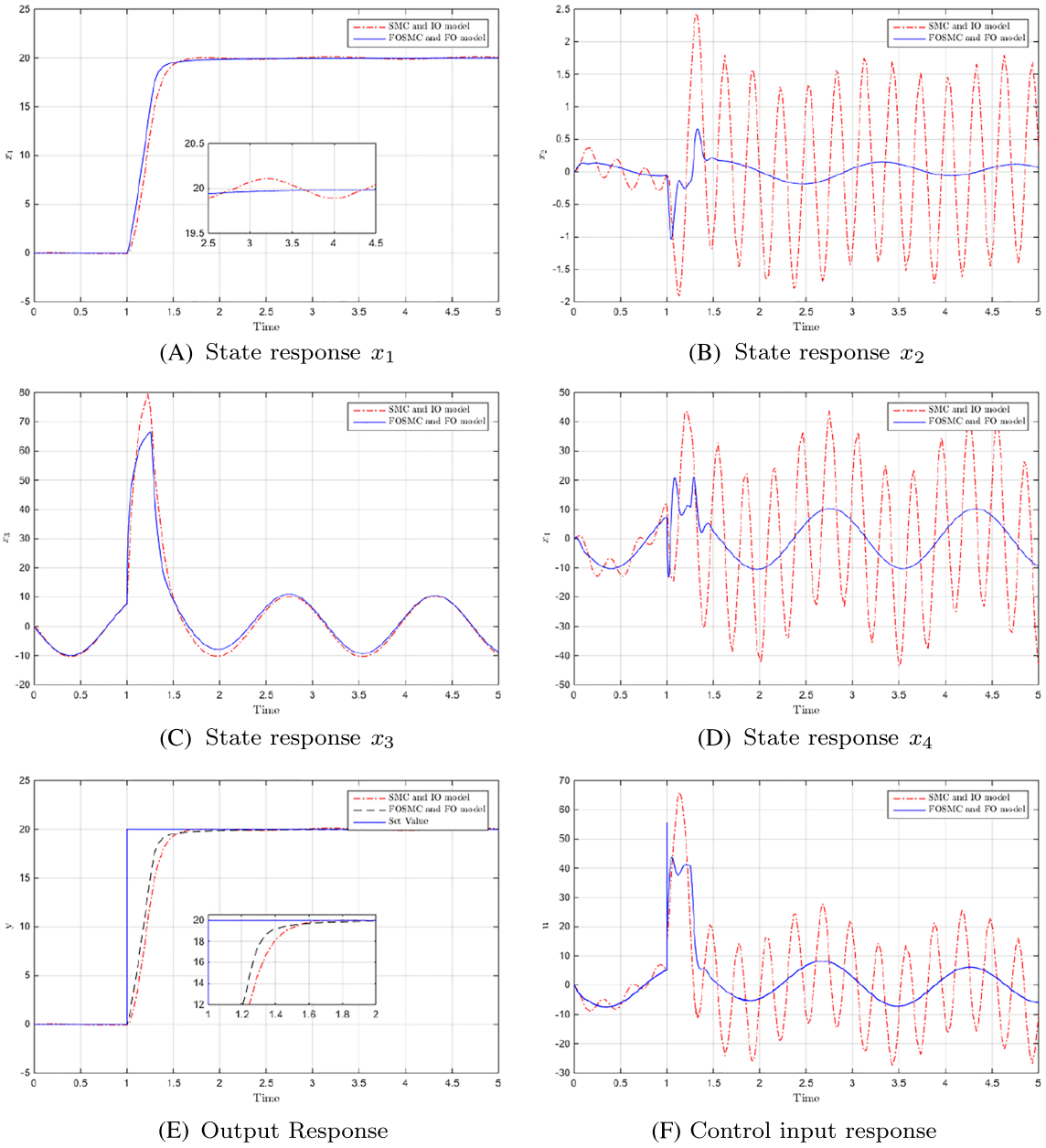

FIGURE 5 Response comparison of FO-SLFM system and IO-SLFM system. FO, fractional order; IO, integer order; SLFM, single-link flexible manipulator [Colour figure can be viewed at wileyonlinelibrary.com]

	Figure 2	Figure 4	Figure 5
Running time, s	2.2	4.1	4.6

TABLE 1 A running time table of the procedures (corresponding to Figures 2, 4, and 5)

5 | CONCLUSION

This paper proposes a FOSMC for a class of noncommensurate fractional-order systems with mismatched disturbances. The contribution of this paper mainly includes three points. First, we process the noncommensurate fractional-order system by splitting it into several subsystems with commensurate order. Second, we designed the fractional-order DOBs for each subsystem in order to estimate the external disturbance. Third, we designed a FOSMC for the noncommensurate fractional-order system based on the DOBs. The proposed FODOB-based FOSMC strategy makes the output tracking the reference without any affection from the external mismatched disturbances. The method has been validated in simulation.

It has high convergence rate and weak chattering. It can be obtained that mathematical modeling of the real physical system with noncommensurate fractional order and the design of the fractional-order controller can achieve higher control accuracy. It has a wide range of application prospects in various sophisticated systems requiring high-precision control. However, when the original system is very complicated or the number of the splitted commensurate subsystems is very high, the loading for design different DOBs is increasing significantly. Is the uniform DOB feasible for dealing with the complicated noncommensurate system? If yes, how to design it? There are still lots of challenges for the perfect control of the noncommensurate system that are worthy of more researchers devoting.

ACKNOWLEDGEMENTS

This work is supported by the National Natural Science Foundation of China (No. 61573050), Fundamental Research Funds for the Central Universities of China (XK1802-4).

CONFLICT OF INTEREST

The authors declared no potential conflicts of interest with respect to the research, authorship, and/or publication of this article.

ORCID

Jing Wang https://orcid.org/0000-0002-6847-8452

REFERENCES

1. Arqub OA. Solutions of time-fractional Tricomi and Keldysh equations of Dirichlet functions types in Hilbert space. *Numer Methods Partial Differ Equ*. 2017;34(5):1759–1780.
2. Arqub OA, Al-Smadi MH. Atangana-Baleanu fractional approach to the solutions of Bagley-Torvik and Painlev equations in Hilbert space. *Chaos Solitons Fractals*. 2018;117:161–167.
3. Arqub OA, Maayah B. Numerical solutions of integrodifferential equations of Fredholm operator type in the sense of the Atangana–Baleanu fractional operator. *Chaos Solitons Fractals*. 2018;117:117–124.
4. El-Taweel TA, Haridy S. An application of fractional factorial design in wire electrochemical turning process. *Int J Adv Manuf Technol*. 2014;75(5-8):1207–1218.
5. Banzhaf CA, Lin LL, Dang N, Freeman M, Haedersdal M, Prow TW. The fractional laser-induced coagulation zone characterized over time by laser scanning confocal microscopy—a proof of concept study. *Lasers Surg Med*. 2018;50(1):70–78.
6. Fournier S, Toth GG, De BB, et al. Six-year follow-up of fractional flow reserve-guided versus angiography-guided coronary artery bypass graft surgery. *Circ Cardiovasc Interv*. 2018;11(6):63–68.
7. Ding D, Liu F, chen H. Sliding mode control of fractional-order delayed memristive chaotic system with uncertainty and disturbance. *Commun Theor Phys*. 2017;68(12):741–749.
8. Arqub OA. Numerical solutions for the Robin time-fractional partial differential equations of heat and fluid flows based on the reproducing kernel algorithm. *Int J Numer Methods Heat Fluid Flow*. 2018;28:828–856.
9. Arqub OA. Fitted reproducing kernel Hilbert space method for the solutions of some certain classes of time-fractional partial differential equations subject to initial and Neumann boundary conditions. *Comput Math Appl*. 2016;73(6):1243–1261.
10. Panteleev AV, Letova TA, Pomazueva EA. Parametric design of optimal in average fractional-order PID controller in flight control problem. *Autom Remote Control*. 2018;79(1):153–166.
11. Yin C, Cheng Y, Chen YQ. Adaptive fractional-order switching-type control method design for 3D fractional-order nonlinear systems. *Nonlinear Dyn*. 2015;82(1):1–14.
12. Wang J, Shao C, Chen Y. Fractional order sliding mode control via disturbance observer for a class of fractional order systems with mismatched disturbance. *Mechatronics*. 2018;53(1):8–19.
13. Utkin VI, Poznyak AS. *Adaptive Sliding Mode Control*. Berlin, Germany: Springer Berlin Heidelberg; 2013.
14. Gao Z, Liao X. Integral sliding mode control for fractional-order systems with mismatched uncertainties. *Nonlinear Dynam*. 2013;72(1-2):27–35.
15. Mujumdar A, Kurode S, Tamhane B. Fractional order sliding mode control for single link flexible manipulator. In: IEEE International Conference on Control Applications; 2013:288–293.
16. Aghababa MP. Design of a chatter-free terminal sliding mode controller for nonlinear fractional-order dynamical systems. *Int J Control*. 2013;86(10):1744–1756.
17. Feng Y, Han F, Yu X. Chattering free full-order sliding-mode control. *Automatica*. 2014;50(4):1310–1314.
18. Mobayen S. An adaptive chattering-free PID sliding mode control based on dynamic sliding manifolds for a class of uncertain nonlinear systems. *Nonlinear Dyn*. 2015;82(1):1–8.

19. Karami-Mollaee A, Tirandaz H, Barambones O. On dynamic sliding mode control of nonlinear fractional-order systems using sliding observer. *Nonlinear Dyn*. 2018;92(3):1379–1393.
20. Oh Y, Wan KC. Disturbance-observer-based motion control of redundant manipulators using inertially decoupled dynamics. *IEEE Trans Mechatron*. 1999;4(2):133–146.
21. Chen WH, Yang J, Guo L, Li S. Disturbance-observer-based control and related methodsan overview. *IEEE Trans Ind Electron*. 2016;63(2):1083–1095.
22. Zhang J, Liu X, Xia Y, Zuo Z, Wang Y. Disturbance observer-based integral sliding-mode control for systems with mismatched disturbances. *IEEE Trans Ind Electron*. 2016;63(11):7040–7048.
23. Li S, Yang J, Chen WH, Chen X. *Disturbance Observer-Based Control: Methods and Applications*. Florida, USA: CRC Press Inc; 2014.
24. Pashaei S, Badamchizadeh M. A new fractional-order sliding mode controller via a nonlinear disturbance observer for a class of dynamical systems with mismatched disturbances. *ISA Trans*. 2016;63:39–48.
25. Jiao Z, Chen YQ. Stability of fractional-order linear time-invariant systems with multiple noncommensurate orders. Pergamon Press Inc; 2012.
26. Mujumdar A, Tamhane B, Kurode S. Observer-based sliding mode control for a class of noncommensurate fractional-order systems. *IEEE/ASME Trans Mechatron*. 2015;20(5):2504–2512.
27. Belkhatir Z, Laleg-Kirati TM. Parameters and fractional differentiation orders estimation for linear continuous-time non-commensurate fractional order systems. *Syst Control Lett*. 2018;115:2633.
28. Trigeassou JC, Maamri N, Oustaloup A. Lyapunov stability of noncommensurate fractional order systems: an energy balance approach. *J Comput Nonlinear Dyn*. 2018;11(4):2101–2111.
29. Gao Z. A graphic stability criterion for non-commensurate fractional-order time-delay systems. *Nonlinear Dyn*. 2014;78(3):2101–2111.
30. Sabatier J, Farges C, Trigeassou JC. A stability test for non-commensurate fractional order systems. *Syst Control Lett*. 2013;62(9):739–746.
31. Monje CA, Chen YQ, Vinagre BM, Xue D, Feliu V. *Fractional-order Systems and Controls*. London: Springer; 2010.
32. Podlubny I. *Fractional Differential Equations*, Mathematics in Science and Engineering. New York,USA: Academic Press; 1999.
33. Wang J. *Control Performance Analysis of Fractional Order System*. Chinese: Electronic Industry Press; 2010.
34. Walsh GC, Ye H, Bushnell LG. Stability analysis of networked control systems. *IEEE Trans Control Syst Technol*. 2002;10(3):438–446.
35. Kurode S, Dixit P. Output feedback control of flexible link manipulator using sliding modes. In: International Conference on Electrical & Computer Engineering; 2013:949–952.
36. Kurode S, Dixit P. Sliding mode control of flexible link manipulator using states and disturbance estimation. *Int J Adv Mechatron Syst*. 2013;5(2):129–137.

How to cite this article: Wang J, Shao C, Chen X, Chen Y. Fractional-order DOB-sliding mode control for a class of noncommensurate fractional-order systems with mismatched disturbances. *Math Meth Appl Sci*. 2021;44:8228–8242. https://doi.org/10.1002/mma.5850